The Effect of the Achilles Tendon on Trabecular Structure in the Primate Calcaneus

SHARON KUO,[1,2]* JEREMY M. DESILVA,[1*] MAUREEN J. DEVLIN,[3] GABRIEL MCDONALD,[4] AND ELISE F. MORGAN[4]

[1]Department of Anthropology, Boston University, 232 Bay State Road, Boston, Massachusetts

[2]Department of Applied Forensic Sciences, Mercyhurst University, 501 E. 38th Street, Erie, Pennsylvania

[3]Department of Anthropology, University of Michigan, 1085 South University Avenue, Ann Arbor, Michigan

[4]Department of Mechanical Engineering, Boston University, 110 Cummington Street, Boston, Massachusetts

ABSTRACT

Humans possess the longest Achilles tendon relative to total muscle length of any primate, an anatomy that is beneficial for bipedal locomotion. Reconstructing the evolutionary history of the Achilles tendon has been challenging, in part because soft tissue does not fossilize. The only skeletal evidence for Achilles tendon anatomy in extinct taxa is the insertion site on the calcaneal tuber, which is rarely preserved in the fossil record and, when present, is equivocal for reconstructing tendon morphology. In this study, we used high-resolution three-dimensional microcomputed tomography (micro-CT) to quantify the microstructure of the trabecular bone underlying the Achilles tendon insertion site in baboons, gibbons, chimpanzees, and humans to test the hypothesis that trabecular orientation differs among primates with different tendon morphologies. Surprisingly, despite their very different Achilles tendon lengths, we were unable to find differences between the trabecular properties of chimpanzee and human calcanei in this specific region. There were regional differences within the calcaneus in the degree of anisotropy (DA) in both chimpanzees and humans, though the patterns were similar between the two species (higher DA inferiorly in the calcaneal tuber). Our results suggest that while trabecular bone within the calcaneus varies, it does not respond to the variation of Achilles tendon morphology across taxa in the way we hypothesized. These results imply that internal bone architecture may not be informative for reconstructing Achilles tendon anatomy in early hominins. Anat Rec, 00:000–000, 2013.

Key words: trabecular bone; Achilles tendon; calcaneus; anisotropy

Grant sponsor: Boston University Undergraduate Research Opportunities Program.

*Correspondence to: Sharon Kuo. E-mail: Sharon0Kuo@gmail.com or Jeremy DeSilva. E-mail: jdesilva@bu.edu

Received 28 July 2012; Accepted 18 May 2013.
DOI 10.1002/ar.22739
Published online in Wiley Online Library (wileyonlinelibrary.com).

TABLE 1. Relative length of Achilles tendon across primates

Species	Tendon length (as % of length of tendon-muscle unit)	Source
Homo sapiens	65%	Frey, 1913
Pan troglodytes	~7.5%	Rauwerdink, 1991[a]
	"Very short"	Urbanowicz and Prejzner-Morawska, 1972
	"Small Achilles tendon"	Myatt et al., 2011
Pan paniscus	10%	Vereecke et al., 2005
	7%	Payne et al., 2006
Gorilla gorilla gorilla	4%	Payne et al., 2006
Gorilla gorilla graueri	0%	Payne et al., 2006
Pongo pygmaeus	18.3%	Myatt et al., 2011
	18%	Payne et al., 2006
Hylobates lar	~45%	Vereecke et al., 2005
	36%	Payne et al., 2006
	~35%	Rauwerdink, 1991[a]
Papio hamadryas	~40%	Rauwerdink, 1991[a]
Macaca mulatta	~25%	Rauwerdink, 1991[a]
Chlorocebus aethiops	~25%	Rauwerdink, 1991[a]
Lagothrix lagotricha	~5%	Rauwerdink, 1991[a]
Ateles spp.	Predominantly "muscular" character	Urbanowicz and Prejzner-Morawska, 1972
Cebus capucinus	~30%	Rauwerdink, 1991[a]

[a]All tendon lengths estimated from Figure 4 of original paper (reported as % of tibia length).

INTRODUCTION

A hallmark of the human lineage is our bipedality. Among the many musculoskeletal anatomies that contribute to human bipedalism is an elongated Achilles tendon (Sellers et al., 2010). The Achilles tendon is comprised of the triceps surae muscle complex merging distally to form a single tendon, which inserts onto the tuber of the calcaneus (O'Brien, 2005; Harris and Peduto, 2006). The Achilles tendon has been found to increase locomotor efficiency by storing energy and returning it in elastic recoil (Alexander and Bennet-Clark, 1977; Alexander, 1984; Ker et al., 1987; Swartz, 1993; Sellers et al., 2010) and is subject to extremely high loads during various activities such as walking, running, and jumping (O'Brien, 2005). Because the Achilles tendon is particularly efficient at storing elastic energy during running, some (e.g., Bramble and Lieberman, 2004) have argued that an elongated tendon was a crucial adaptation that allowed for long distance endurance running in early members of the genus *Homo*.

Modern humans have the longest Achilles tendon relative to total muscle length of any living primate (Table 1), comprising approximately 65% of the total muscle length (Frey, 1913; Vereecke et al., 2005). In contrast, most other apes have a short tendon and their muscle mass is located more distally in the leg (Crompton et al., 2010). In chimpanzees, for example, the Achilles tendon constitutes a small percentage (~7.5%) of the total muscle length (Table 1). This small tendon-to-muscle ratio permits a greater ankle joint excursion (Hanna and Schmidt, 2011; Myatt et al., 2011), which may permit the extreme dorsiflexion exhibited during vertical climbing in the apes (DeSilva, 2009). Interestingly, however, gibbons (*Hylobates*) have a relatively long Achilles tendon compared to the other nonhuman apes (~35–45% of total muscle length) (Table 1). Although they are primarily arboreal brachiators, gibbons occasionally walk on their hind legs both terrestrially and arboreally (McCann, 1933; Sati and Alfred, 2002; Vereecke et al., 2006; Payne et al., 2006).

It is currently unclear when, during the course of human evolution, the Achilles tendon lengthened (Sellers et al., 2010). In fact, given the pattern of relative Achilles tendon lengths (Table 1) in primates, it remains possible that an elongated tendon is the ancestral condition and the great apes independently evolved larger muscle/tendon ratios as adaptations to vertical climbing (e.g., Lovejoy et al., 2009). Alternatively, some have suggested that an elongated Achilles may be an adaptation that developed in the genus *Homo* (Bramble and Lieberman, 2004; Lieberman et al., 2009). However, this hypothesis is difficult to test since a systematic comparison of the external anatomy of the calcaneus has yet to reveal an obvious skeletal correlation with Achilles tendon length. Though the Achilles tendon does leave evidence of its insertion on the calcaneal tuber, efforts to determine Achilles tendon length using such external markers have yielded mixed results, thereby limiting our ability to quantify its length based on fossilized bones (Bramble and Lieberman, 2004; Zipfel et al., 2011). For example, it is unclear whether *Australopithecus* had an elongated Achilles tendon based on external morphology (Bramble and Lieberman, 2004). Zipfel et al. (2011) found that the *Au. sediba* calcaneus (U. W. 88–99) possessed some similarities with modern humans related to the Achilles tendon insertion area, namely a smooth sloped surface for the retrocalcaneal bursa and well-developed ossified Sharpey's fibers at the Achilles enthesis. These anatomies are thought to indicate the presence of a long Achilles tendon, as they are present on human calcanei and absent on chimpanzee calcanei (Zipfel et al., 2011), but as the authors note, some of these features can be found in a small number of gorilla calcanei, which possess very short Achilles tendons (Table 1).

Complicating these efforts to reconstruct the natural history of the hominin Achilles is the near absence of

TABLE 2. Complete record of calcanei currently known in the fossil record

Specimen identification	Species	Age	State of preservation	Achilles enthesis preserved	Source
ARA-VP-6/500-96	*Ardipithecus ramidus*	4.4 Ma	4 pieces of subtalar facet		White et al., 2009
DIK-1-1F	*Australopithecus afarensis*	3.3 Ma	Juvenile tuber: unfused		Alemseged et al. 2006
A.L. 333-8	*Au. afarensis*	3.2 Ma	Well preserved with minor erosion along tuber. Damaged anteriorly	X	Latimer et al. 1982
A.L. 333-37	*Au. afarensis*	3.2 Ma	Posterior half preserved, superiomedial tuber absent	X	Latimer et al. 1982
A.L. 333-55	*Au. afarensis*	3.2 Ma	Well preserved; damaged anteriorly, minor erosion along tuber	X	Latimer et al. 1982
StW 573	*Au.* sp.	~3 Ma	Fragment only preserving talar facets		Deloison 2003
StW 352	*Au. africanus*	2.0-2.6 Ma	Articulation for cuboid and talus preserved but posterior region absent		Deloison 2003
StW 363	*Au. africanus*	2.0-2.6 Ma	Small fragment		Fisk & Macho 1992
Omo 33-74-896	*Homo*?	2.36 Ma	Relatively complete except for extensive damage on tuber		Gebo & Schwartz 2006
U.W. 88-99	*Au. sediba*	1.977 Ma	Complete calcaneus, minor erosion anteriorly	X	Zipfel et al. 2011
U.W. 88-113	*Au. sediba*	1.977 Ma	Isolated apophysis	X	Zipfel et al. 2011
KNM-ER 1500	*Paranthropus boisei*?	1.89 Ma	Heavily eroded fragment		Day et al. 1976
OH 8	*H. habilis*? *P. boisei*?	1.85 Ma	Articulation for cuboid and talus preserved but posterior region absent		Day & Napier 1964
KB 3297	Identified as *P. robustus*, Probably cercopithecoid	l.75 Ma	Articulation for cuboid and talus preserved but posterior region absent		Thackeray et al. 2001

fossil calcanei that preserve the calcaneal tuber (Table 2). The majority of fossil calcanei discovered have substantial damage to the area where the Achilles tendon inserts, thereby limiting the number of fossils that could potentially shed light on the evolution of this structure. Some researchers have therefore suggested that evidence for an elongated tendon may be found in the internal microstructure of the calcaneus (Crompton et al., 2010; Sellers et al., 2010). Maga et al. (2006) examined the trabecular architecture of the calcaneus in several hominoid species and found important, perhaps functionally relevant, differences. However, the sample sizes were too small to draw statistically significant conclusions, and the volume of interest was selected to study the overall stresses on the proximal calcaneus, rather than focusing specifically on the tensile pull of the Achilles tendon. In this study, we limited our volume of interest (VOI) to the trabecular bone directly underlying the tendon insertion on the calcaneal tuber since this bone should be most sensitive to the tensile strains produced during the contraction of the triceps surae.

Wolff's "Law" (Wolff, 1892) postulates that bone responds and adapts to its loading environment. Under this assumption, differences in strain (frequency or magnitude) are expected to yield differences in trabecular microarchitecture. There have been very few studies that test specifically whether the Achilles tendon has an impact on trabecular bone. In one such study, Biewener et al. (1996) investigated the effect that Achilles tendon removal had on the trabecular bone in potoroos (a small marsupial). They compared the trabecular architecture of a disuse group with an excised Achilles tendon to a control group of active adult potoroos. In accordance with the expectation of bony functional adaptation, Biewener et al. (1996) found that trabecular bone underlying the Achilles insertion differed substantially between the two groups, with Tb.N (/mm), Tb.Th (mm), and BV/TV (%) (see Table 3 for definitions) significantly lower in the disuse group. Interestingly, the degree of anisotropy (DA) did not differ between the groups, suggesting to Biewener et al. (1996) that the DA of trabecular bone in a given area may be established early in

TABLE 3. Trabecular properties analyzed and definitions of each

Property	Abbreviation	Definition
Bone volume fraction	BV/TV	Ratio of bone volume to total volume
Trabecular number	Tb.N	Average number of trabecular struts per unit length (/mm)
Trabecular thickness	Tb.Th	Average thickness of a trabecular strut (mm)
Degree of anisotropy	DA	Maximum to minimum mean intercept length value (Whitehouse 1974), or preferential directionality
Principal trabecular orientation	PTO	Angulation of the principal trabeculae from the long axis of the calcaneus

development and is not as responsive to disuse. To what degree the trabecular bone underlying the Achilles responds to *increased* use instead of disuse is unclear and is yet to be experimentally evaluated. These findings (Biewener et al., 1996) tentatively suggest that variation in Achilles tendon anatomy could result in different trabecular architecture in the calcaneus. If so, it is reasonable to hypothesize that primates with longer Achilles tendons should have quantifiable differences in the trabecular architecture underlying the tendon compared to primates with shorter tendons, since the longer tendons may exert more directed tensile forces on the bone. Specifically, the orientation of the trabeculae might be more unidirectional in long-tendoned primates than short-tendoned primates due to the pull of the tendon (Fig. 1). Conversely, a distal muscle belly attached to a short, broad tendon may exert a more multidirectional pull (Fig. 1), though this has never been experimentally demonstrated.

Microcomputed tomography (micro-CT) allows researchers to quantify the complex three-dimensional geometry of trabecular bone and may shed light on this problem. Micro-CT is often used to assess microarchitecture of both cortical and trabecular bone (Bouxsein et al., 2010). We hypothesize that properties of trabecular bone, namely BV/TV, Tb.N, Tb.Th, and especially DA and PTO (Table 3) will differ in primates with different relative Achilles tendon lengths. Our hypotheses for this study are as follows:

H_0: Variation in the Achilles tendon produces no discernible effect on the trabecular bone of the primate calcaneus.

H_1: Variation in Achilles tendon anatomy among primates will correspond to differences in the morphology of the bone underlying the tendon insertion in the posterior calcaneus.

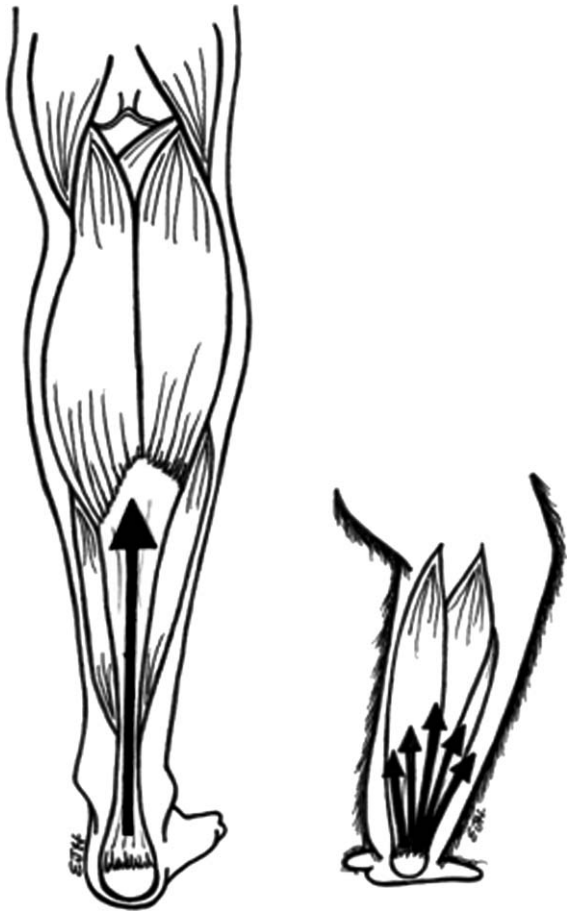

Fig. 1. Unidirectional pull of the long Achilles tendon in humans (left) and multidirectional pull of the short Achilles tendon in chimpanzees (right). Illustration by Emory Holland.

METHODS

Specimens

Seven cadaveric *Homo sapiens* calcanei were obtained from Boston University's medical campus. These calcanei were all from adults, but sex, exact age, and activity patterns are unknown. The calcanei were sectioned coronally at the superior most aspect of the talar articular surface so that they would fit into the micro-CT scanner.

Nonhuman primate calcanei were borrowed from the Harvard Museum of Comparative Zoology (MCZ). The sample was comprised of four baboons (*Papio* spp.), six gibbons (*Hylobates lar*), and four chimpanzees (*Pan troglodytes*). All were adult, wild-shot individuals (Table 4).

TABLE 4. Specimen list, separated by sex

Species	Male	Female	Unknown	Total
Papio spp.	2	0	2	4
Hylobates lar	3	3	0	6
Pan troglodytes	3	1	0	4
Homo sapiens	0	0	7	7

Scanning

Two scanners were used in this study due to size differences of the primate calcanei: a micro-CT 40

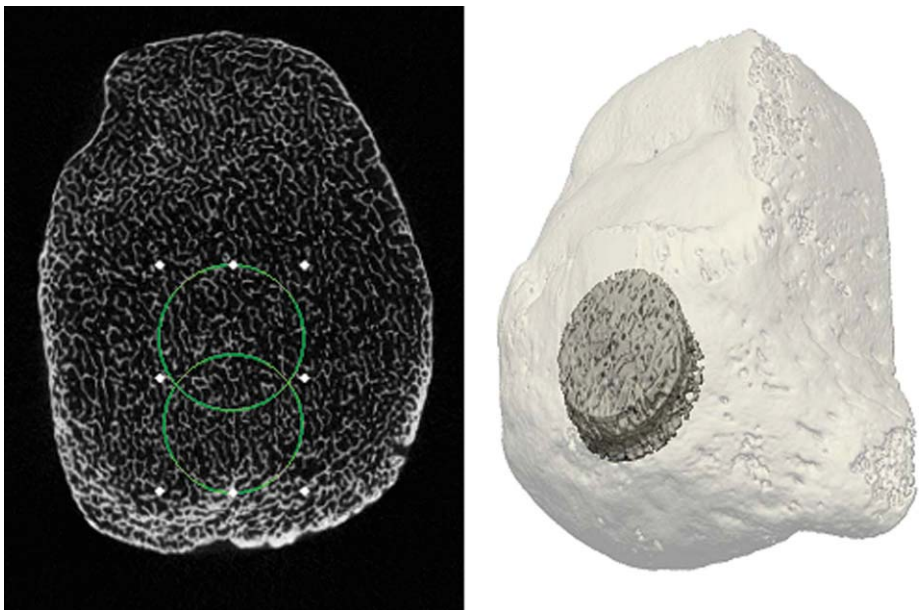

Fig. 2. Location of contoured areas demonstrated in a human calcaneus. Left: 25% (higher circle) and 10% (lower circle) contours. Right: a three-dimensional visualization of the 25% volume of interest for a human calcaneus (shown obliquely such that the posterior and lateral portion of the bone is visible). Notice that the VOI is just inferior to the ossified Sharpey's fibers that delineate the insertion of the Achilles tendon.

(SCANCO Medical, Brüttisellen, Switzerland) at the Center for Advanced Orthopaedic Studies (Beth Israel Deaconess Medical Center, Harvard Medical School), and a micro-CT 80 (SCANCO Medical, Brüttisellen, Switzerland) at the Department of Mechanical Engineering at Boston University. Both locations use SCANCO software to evaluate and quantify bony microarchitecture. Separating the four taxa into two groups (gibbon v. baboon; human v. chimpanzee) minimized complications related to size differences, but prevented comparisons between the two groups.

Baboon and gibbon calcanei were scanned in the micro-CT 40. Our goal in this part of the study was to compare the trabecular architecture of similarly sized primates with Achilles of similar lengths (Table 1) to test whether different locomotor patterns alone can explain trabecular differences. Gibbons are arboreal brachiators that also occasionally travel bipedally (Vereecke et al., 2006), whereas baboons travel quadrupedally on a semiplantigrade foot, and are primarily terrestrial (Rose, 1977). Small foam pieces were used to hold the calcanei in place during scanning. The outer circumference of each foam piece was cut to be the size of the scanning tube (36.9 mm). A hole was cut in the inside of the foam piece, forming a doughnut-like shape, into which the specimen was placed. The specimen was oriented so that a line connecting the superior most aspect of the talar articular surface to the superior most aspect of the calcaneal tuber was parallel with the vertical line of the scanning tube. The calcaneus was placed perpendicular to the scanning plane with the calcaneal tuber positioned superiorly. In scout view, half of the distance between the superior most talar articular surface and the most proximal part of the calcaneal tuber was selected so that homologous regions of the bone were represented in the different taxa (following Fajardo and Müller, 2001). The average number of slices scanned for baboons was 341 slices and 169 slices for gibbons. All baboons and gibbons were scanned at medium resolution, 70 kVp, 114 μA.

Chimpanzee and human calcanei were scanned in a micro-CT 80. These specimens were scanned in a 61.4 mm tube and oriented as described for the baboon and gibbon specimens. Again, a region comprising half of the distance between the posterior-most aspect of the calcaneal tuber and the superior-most aspect of the talar articular surface (or, in the case of the human specimens, the site of sectioning) was selected for scanning. The average number of slices scanned was 231 slices for chimpanzees and 282 slices for humans. All chimpanzee and human calcanei were scanned at medium resolution (60 μm), 70 kVp, 114 μA.

Contouring

The scans were contoured to isolate the region of trabecular bone hypothesized to be most influenced by the pull of the Achilles tendon. Scans were oriented so that coronal plane slices could be contoured. Contouring of the trabecular VOI began at the first slice in which trabecular bone was clearly seen and a shell of cortical bone was restricted to the external perimeter of the calcaneus (cortical bone was not included in the contoured VOI). The maximum length and width of the slice were taken. A region 25% of the length away from the inferior border of the calcaneus was located and a circular contour was made (Fig. 2). Ideally, the circle would also be exactly 25% of the length away from the inferior and horizontal edges, but due to the irregular, vertically oblong shape of the calcaneus in some of the specimens (especially gibbons), the circle was closer to the

TABLE 5. Trabecular properties for all specimens at the 25% VOI

Species	Total length	BV/TV	Tb.N	Tb.Th	DA
Papio spp.	49±1.0	0.40±.068	2.1±.17	0.22±.047	1.9±.19
Hylobates lar	25±1.1	0.37±.10	2.3±.38	0.20±.039	1.9±.25
P-value		0.57	0.26	0.38	0.88
Pan troglodytes	54±3.0	0.14±.10	1.5±.46	0.20±.044	1.2±.10
Homo sapiens	76±5.7	0.26±.085	1.8±.27	0.22±.036	1.3±.10
P-value		0.07	0.23	0.30	0.15

P-values for baboon/gibbon and chimpanzee/human comparisons are provided with significance determined at $P<0.05$.

mediolateral sides of the calcaneus. Contouring continued until half the number of slices scanned was reached ensuring that the bone quantified was comprised of the trabeculae nearest to the Achilles insertion. These methods resulted in a different number of contoured slices between specimens, but the same proportional region of each calcaneus by length (the posterior quarter of each specimen), as recommended elsewhere (Fajardo and Müller, 2001).

In addition to the 25% central location of the first contour, we did a second set of contours in chimpanzees and humans. These were made by simply moving the contours in an inferior direction (plantarly) so that the margin of the circular contour was 10% away from the inferior border of each slice of calcaneus (Fig. 2). Similar to the 25% contours, we continued until half the number of slices scanned was reached. This was done to add a second volume of interest (VOI) to the study, as X-rays and resin slices of humans (Milz et al., 2002) indicated that trabeculae located more inferior to the Achilles tendon insertion may be more oriented, and the tensile pull of the Achilles tendon may have a greater effect on this region.

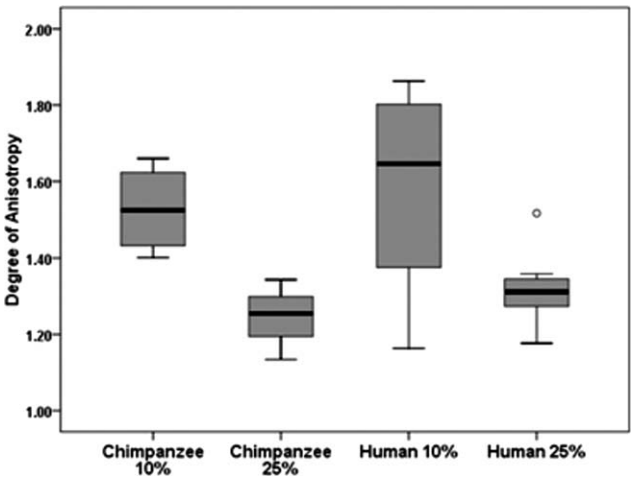

Fig. 3. Average degree of anisotropy of chimpanzee and human calcanei at the 25% region versus the 10% region. Significant differences were found between the 25% region and 10% region degree of anisotropy in both taxa. However, there were no statistically significant differences in DA between humans and chimpanzees for homologous 10 and 25% VOIs. Boxplots are shown here with the median (black bars), interquartile range (gray boxes) and full ranges (whiskers). Outliers are shown as unfilled circles.

Thresholds and Evaluation

Contours were evaluated using SCANCO software. An adaptive iterative thresholding (AIT) program was used to determine the ideal threshold for each specimen following the methodology of previous studies (Ridler and Calvard, 1978; Trussel, 1979; Ryan and Ketcham, 2002; Maga et al., 2006; Fajardo et al., 2007; DeSilva and Devlin, 2012). In the event that the two taxa being compared did not have statistically different thresholds, they were evaluated at one fixed threshold, which was the average of the two taxa. In the event that the two taxa being compared were different, each taxon was evaluated at its own ideal threshold. Statistical analysis was done using SPSS (IBM Corp., Armonk, NY). Because of small sample sizes, we used nonparametric statistics. Trabecular parameters were compared between species using a Mann–Whitney U-test while comparisons within calcanei between the 25 and 10% VOI were statistically evaluated using a paired Wilcoxon test.

The thresholds for the baboons and gibbons were not significantly different ($P = 0.14$); thus we used a fixed mean threshold for both taxa. The thresholds for the human and chimpanzee specimens were different from each other ($P = 0.02$). We therefore ran the analyses at each taxon's mean threshold, reported below. We also compared humans and chimpanzees at their fixed mean threshold and found similar results (data not shown).

RESULTS

There were no differences in the trabecular properties between baboons and gibbons (Table 5). In fact, the two taxa had nearly identical trabecular architecture in the calcaneal tuber despite having very different locomotive patterns. Surprisingly, no differences were found in the trabecular microarchitecture of chimpanzee and human calcanei either (Table 5; Fig. 3).

In the 10% region of chimpanzee and human calcanei, there were also no differences in the trabecular properties of the two taxa (Table 6). However, there was a difference in DA between the two regions (25% VOI and 10% VOI) in humans ($P = 0.03$) and a strong trend towards a difference in chimpanzees ($P = 0.06$) (Fig. 3).

We found *post hoc* that in gibbons, trabecular properties differed between males and females. Males had higher BV/TV values than females ($P = 0.0001$). Unfortunately, due to an insufficient number of female specimens in the other taxa (or, in the case of the humans, a lack of sex identification), we were unable to run similar tests on the remaining specimens.

TABLE 6. Average BV/TV, Trabecular number, trabecular thickness, and degree of anisotropy for chimpanzee and human specimens at 10% VOI with *P*-values

Species	BV/TV	Tb.N	Tb.Th	DA
Pan troglodytes	0.20 ± .12	1.6 ± .44	0.25 ± .02	1.53 ± .12
Homo sapiens	0.30 ± .11	1.8 ± .33	0.24 ± .04	1.58 ± .29
P-value	0.11	0.53	0.79	0.65

DISCUSSION

The purpose of this study was to determine whether trabecular bone architecture in the calcaneus reflects Achilles tendon length variation in four different primates. Our results fail to reject the null hypothesis, suggesting that internal microarchitecture of the calcaneal trabeculae may not correlate with Achilles tendon length as we predicted.

Baboons and gibbons were compared due to their different forms of locomotion, but similar Achilles tendon lengths. A terrestrial, semiplantigrade quadruped (baboon) most likely has different loads on its calcaneus than an arboreal brachiator (gibbon), yet there were no differences in the trabecular properties of the bone underlying their Achilles tendon insertion sites. This similarity suggested to us that the similar Achilles tendon lengths of these two primates (Table 1) may be responsible for the similar trabecular architecture. If so, then humans and chimpanzees should have quite different trabecular properties given their different Achilles tendon lengths. Yet, the analysis of the trabecular bone in the calcanei of these taxa revealed no differences. The similarity in DA between humans and chimpanzees ($P = 0.16$ in the 25% region; $P = 0.65$ in the 10% region) was surprising since the Achilles tendon was predicted to have the greatest effect on this aspect of the trabecular architecture. Additionally, we calculated the angle of the principal trabecular orientation (PTO) to test whether the actual direction of the trabeculae differed between specimens, but found no significance between chimpanzees and humans ($P = 0.23$). We did find a difference in the DA of trabeculae between the 25% region vs. the 10% region of the same calcaneus. We found that there was a difference between the DA of the two regions in humans ($P = 0.03$) and a near significant difference in chimpanzees ($P = 0.06$), indicating that trabecular orientation does vary within the calcaneus; however, an identical pattern is found in both humans and chimpanzees.

Recently, both Sellers et al. (2010) and Crompton et al. (2010) suggested that evidence for a lengthy Achilles tendon may be found in the trabecular microarchitecture underlying the Achilles insertion. We agreed with these authors that studying the Achilles tendon's effect on trabeculae was an appropriate approach and attempted to test this hypothesis in a small sample of primates; however, our study failed to find any correlation between Achilles tendon morphology and parameters of trabecular microstructure in the region underlying the Achilles tendon. The evolution of the Achilles tendon therefore remains an open question. From the results of this study, we cannot discern the Achilles length or direction of pull based on the trabecular bone in the calcaneal tuber. Our failure to reject the null hypothesis could be due to the small sample sizes or the high degree of variation present in each taxon. For example, we found that there is a difference ($P = 0.0001$) between male and female gibbon BV/TV. We were only able to observe this in gibbons, as the other taxa either did not have enough specimens of both sexes, or the sex was unknown. We suggest that the difference in trabecular properties between the sexes may play a role in the substantial intraspecific variation (Hudelmaier et al., 2005; Eckstein et al., 2007). Though our volumes of interest were chosen to specifically isolate trabeculae that would be most impacted by the Achilles, there is a possibility that these VOIs were not in the correct locations or the correct size. Furthermore, we only tested four primate species and perhaps a broader interspecific study would yield different results. We would recommend that future researchers divide specimens by sex to decrease intraspecific variation, which may have been too extensive to see a clear pattern in this study.

There is also the possibility that the tensile strain produced at the junction of the Achilles tendon and the calcaneus has a stronger influence on the cortical bone than the trabecular bone. The focus of this study was trabecular bone, but we can preliminarily report that the cortical bone thickness directly overlying the trabecular VOI appears to be thicker in chimpanzees than in humans (Fig. 4). Although these data are consistent with other findings that apes tend to have thicker cortical bone than humans (Cotter et al., 2009), they are unexpected if tensile forces produced by the Achilles were influencing cortical thickness. Along these same lines, we do find one aspect of our negative results as potentially illuminating and worthy of further consideration. Comparative studies characterizing the microarchitecture of trabecular bone have consistently found that humans have a lower bone volume fraction (BV/TV) than chimpanzees. Whether in the humeral head (Shaw and Ryan, 2012; Scherf et al., 2013), first metacarpal head (Lazenby et al., 2011), thoracic vertebra (Cotter et al., 2011), femoral head (Shaw and Ryan, 2012), calcaneal body (Maga et al., 2006), talar body (DeSilva and Devlin, 2012), or medial metatarsal heads (Griffin et al., 2010), humans consistently possess lower BV/TV than chimpanzees. Under the Achilles tendon insertion, however, we found a trend towards slightly higher BV/TV in humans than in chimpanzees, though this trend was not statistically significant. The fact that humans have equal (and, if anything, greater) bone volume fraction than chimpanzees in the region underlying the Achilles is curious, given what appears to be a global pattern of reduced BV/TV in the human skeleton. We encourage future work investigating this observation in more detail.

Nevertheless, our study preliminarily suggests that varying Achilles tendon anatomy does not affect the underlying bone in primates as we suspected. One possible explanation for these results is that our model proposing that calcaneal loading direction differs in primates with long versus short Achilles tendons is incorrect or overly simplistic. Another possibility is that the forces at the Achilles tendon insertion have the same magnitude and direction regardless of tendon length, leading to an absence of differences in trabecular morphology at the enthesis. Experimental data on the Achilles/calcaneal junction are sorely needed to assess the validity of our

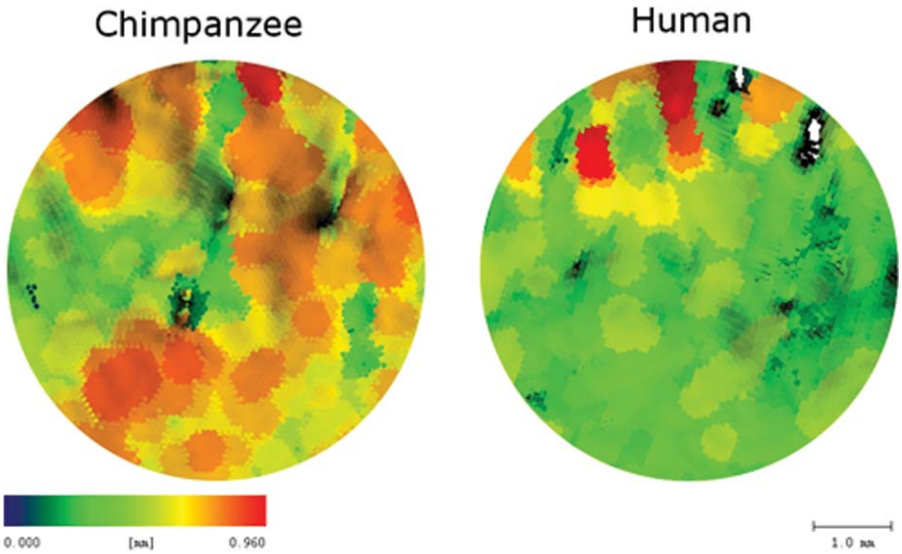

Fig. 4. Cortical bone thickness in the region directly overlying the trabecular VOI in a chimpanzee (left) and human (right). The cortex is thicker (orange and red colors) in the ape, but thinner in the human (green). These findings were consistent in the three chimpanzee and two human calcanei for which these measurements were possible. Though these data should be regarded as preliminary, they are nonetheless contrary to predictions that tensile pull of the Achilles tendon would promote cortical bone growth.

model. Alternatively, if our model for how the Achilles tendon loads calcaneal trabecular bone is correct, then our findings contradict some predictions of Wolff's "Law." Although many have found evidence for trabecular bone adaptation to changes in diet and hormones (Hodgkinson et al., 1978; Reeve et al., 1980; Devlin et al., 2010), and loading (Pontzer et al., 2006; Barak et al., 2011), others (Fajardo et al., 2007; Ryan and Walker, 2010; Shaw and Ryan, 2012; DeSilva and Devlin, 2012) have found the relationship between trabecular bone and inferred mechanical loading in primates to be more complicated. Although trabecular bone clearly is responsive to a variety of factors, Achilles tendon length may not affect trabecular properties as we had predicted.

CONCLUSION

In this study, we tested whether differing Achilles tendons in primates could be detected in the trabecular microarchitecture underlying the tendon insertion. Surprisingly, we failed to find differences in any trabecular bone parameter. These findings suggest that internal bone anatomy is not particularly useful in reconstructing tendon morphologies, thereby limiting its utility in reconstructing tendon length in extinct hominins. Thus, the evolutionary history of the Achilles tendon remains an open question.

ACKNOWLEDGEMENTS

The authors would like to thank Judy Chupasko at Harvard University's Museum of Comparative Zoology for loaning the non-human calcanei and Dr. Donald Siwek at Boston University's Forensic Anthropology Program for the use of the human calcanei. They are grateful to Beth Israel Deaconess Medical Center for the use of their micro-CT 40 scanner and Boston University Department of Mechanical Engineering for the use of their micro-CT 80 scanner. They are extremely grateful to Mary Bouxsein, Leeann Louis, Esther Zusstone, Cheyenne Lewis, and Matthew Reichert for their invaluable assistance and input. Emory Holland's artistic talent is on display in Fig. 1. They are grateful to Scott Miller and two anonymous reviewers for insightful comments that helped improve the manuscript. This project was funded by the Boston University Undergraduate Research Opportunities Program.

LITERATURE CITED

Alemseged Z, Spoor F, Kimbel WH, Bobe R, Geraads D, Reed D, Wynn JG. 2006. A juvenile early hominin skeleton from Dikika, Ethiopia. Nature 443:296–301.

Alexander R M. 1984. Walking and Running: Legs and leg movements are subtly adapted to minimize the energy costs of locomotion. Am Sci 72:348–354.

Alexander RM, Bennet-Clark HC. 1977. Storage of elastic strain energy in muscle and other tissues. Nature 265:114–117.

Barak MM, Lieberman DE, Hublin J. 2011. A Wolff in sheep's clothing: Trabecular bone adaptation in response to changes in joint loading orientation. Bone 49:1141–1151.

Biewener AA, Fazzalari NL, Konieczynski DD, Baudinette RV. 1996. Adaptive changes in trabecular architecture in relation to functional strain patterns and disuse. Bone 19:1–8.

Bouxsein ML, Boyd SK, Christiansen BA, Guldberg RE, Jepsen KJ, Muller R. 2010. Guidelines for assessment of bone microstructure in rodents using micro–computed tomography. J Bone Miner Res 25:1468–1486.

Bramble DM, Lieberman DE. 2004. Endurance running and the evolution of *Homo*. Science 432:345–352.

Cotter MM, Loomis DA, Simpson SW, Latimer B, Hernandez CJ. 2011. Human evolution and osteoporosis-related spinal fractures. PLoS One 6:e26658.

Cotter MM, Simpson SW, Latimer BM, Hernandez CJ. 2009. Trabecular microarchitecture of hominoid thoracic vertebrae. Anat Rec 292:1098–1106.

Crompton RH, Sellers WI, Thorpe SKS. 2010. Arboreality, terrestriality, and bipedalism. Phil Trans R Soc B 365:3301–3314.
Day MH, Leakey REF, Walker AC, Wood BA. 1976. New hominids from East Turkana, Kenya. Am J Phys Anthropol 45:369–435.
Day MH, Napier JR. 1964. Hominid fossils from Bed I, Olduvai Gorge, Tanganyika: Fossil foot bones. Nature 201:969–970.
Deloison Y. 2003. Anatomie des os fossils de pieds des hominids d'Afrique du sud dates entre 2,4 et 3,5 millions d'annés. Interprétation quant à leur mode de locomotion. Biom Hum Anthropol 21:189–230.
DeSilva JM. 2009. Functional morphology of the ankle joint and the likelihood of climbing in early hominins. Proc Natl Acad Sci 106: 6567– 6572.
DeSilva JM, Devlin MJ. 2012. A comparative study of the trabecular bony architecture of the talus in humans, non-human primates, and *Australopithecus*. J Hum Evol 63:536–551.
Devlin MJ, Cloutier AM, Thomas NA, Panus DA, Lotinun S, Pinz I, Baron R, Rosen CJ, Bouxsein ML. 2010. Caloric restriction leads to high marrow adiposity and low bone mass in growing mice. J Bone Miner Res 25:2078–2088.
Eckstein F, Matsuura M, Kuhn V, Priemel M, Müller R, Link TM, Lochmüller E. 2007. Sex differences of human trabecular bone microstructure in aging are site-dependent. J Bone Miner Res 22: 817–824.
Fajardo R, Müller R. 2001. Three-dimensional analysis of nonhuman primate trabecular architecture using micro-computed tomography. Am J Phys Anthropol 115:327–336.
Fajardo R, Müller R, Ketcham R, Colbert M. 2007. Nonhuman anthropoid primate femoral neck trabecular bone and its relationship to locomotor mode. Anat Rec 290:422–436.
Fisk GR, Macho GA. 1992. Evidence of a healed compression fracture in a Plio-Pleistocene hominid talus from Sterkfontein, South Africa. Int J Osteoarch 2:325–332.
Frey H. 1913. Der Musculus triceps surae in der Primatenreihe. Morph Jahrb 47:1–192.
Gebo D L, Schwartz GT. 2006. Foot bones from Omo: Implications for hominid evolution. Am J Phys Anthropol 129:499–511.
Griffin NL, D'Août K, Ryan TM, Richmond BG, Ketcham RA, Postnov A. 2010. Comparative forefoot trabecular bone architecture in extant hominids. J Hum Evol 59:202–213.
Hanna J B, Schmitt D. 2011. Comparative triceps surae morphology in primates: A review. Anat Res Int 2011:1–22.
Harris CA, Peduto AJ. 2006. Achilles tendon imaging. Aust Radiol 50:513–525.
Hodgkinson A, Aaron JE, Horseman A, McLachlan MSF, Nrodin BE. 1978. Effect of oophorectomy and calcium deprivation on bone mass in the rat. Clin Sci Mol Med 54:439–446.
Hudelmaier M, Kollstedt A, Lochmüller EM, Kuhn V, Eckstein F, Link TM. 2005 Gender differences in trabecular bone architecture of the distal radius assessed with magnetic resonance imaging and implications for mechanical competence. Osteoporos Int 16:1124–33.
Ker RF, Bennett MB, Bibby SR, Kester RC, Alexander RM. 1987. The spring in the arch of the human foot. Nature 325:147–149.
Latimer BM, Lovejoy CO, Johanson DC, Coppens Y. 1982. Hominid tarsal, metatarsal, and phalangeal bones recovered from the Hadar formation: 1974–1977 collections. Am J Phys Anthropol 57: 701–719.
Lazenby RA, Skinner MM, Hublin JJ, Boesch C. 2011. Metacarpal trabecular architecture variation in the chimpanzee (*Pan troglodytes*): Evidence for locomotion and tool-use? Am J Phys Anthropol 144:215–222.
Lieberman CO, Bramble DM, Raichlen DA, Shea JJ. Brains, brawn, and the evolution of human endurance running capabilities. In: Frederick EG, John GF, Richard EL, editor. The first humans: Origin and early evolution of the genus *Homo*. New York: Springer, 2009.
Lovejoy CO, Latimer B, Suwa G, Asfaw B, White TD. 2009. Combining prehension and propulsion: The foot of *Ardipithecus ramidus*. Science 326:72.
Maga M, Kappelman J, Ryan TM, Ketcham RA. 2006. Preliminary observations on the calcaneal trabecular microarchitecture of extant large-bodied hominoids. Am J Phys Anthropol 129:410–417.
McCann C. 1933. Notes on the colouration and habits of the white-browed gibbon or hoolock (*Hylobates hoolock* Harl.) J Bombay Nat Hist Soc 36:395–405.
Milz S, Rufai A, Buettner A, Putz R, Ralphs JR, Benjamin M. 2002. Three-dimensional reconstructions of the Achilles tendon insertion in man. J Anat 200:145–152.
Myatt J P, Schilling N, Thorpe SKS. 2011. Distribution patterns of fibre types in the triceps surae muscle group of chimpanzees and orangutans. J Anat 218:402–412.
O'Brien M. 2005. The anatomy of the Achilles tendon. Foot Ankle Clin 10:225–238.
Payne R, Crompton RH, Isler K, Savage R, Vereecke EE, Günther MM, Thorpe SKS, D'Août K. 2006. Morphological analysis of the hindlimb in apes and humans. J Anat 208:709–724.
Pontzer H, Lieberman DE, Momin E, Devlin MJ, Polk JD, Hallgrimsson B, Cooper DML. 2006. Trabecular bone in the bird knee responds to high sensitivity to changes in load orientation. J Exp Biol 209:57–65.
Rauwerdink GP. 1991. Muscle fiber and tendon lengths in the distal limb segments of primates. Z Morphol Anthropol 78:331–340.
Reeve J, Meunier PJ, Parsons JA, Bernat M, Bijvoet OLM, Courpron P, Edouard C, Klenerman L, Neer RM, Renier JC, Slovik D, Vismans FJFE, Potts JT. 1980. Anabolic effect of human parathyroid hormone fragment on trabecular bone in involutional osteoporosis: A multicentre trial. Brit Med J 1340–1344.
Ridler S, Calvard TW. 1978. Picture thresholding using an iterative selection method. IEEE Trans Syst Man Cybern 8:630–632.
Rose MD. 1977. Positional behaviour of olive baboons (*Papio anubis*) and its relationship to maintenance and social activities. Primates 18:59–116.
Ryan T, Walker A. 2010. Trabecular bone structure in the humeral and femoral heads of anthropoid primates. Anat Rec 293:719–729.
Ryan TM, Ketcham RA. 2002. Femoral head trabecular bone structure in two omomyid primates. J Hum Evol 42:241–263.
Sati JP, Alfred JRB. 2002. Locomotion and posture in Hoolock gibbon. Ann For 10:298–306.
Scherf H, Harvati K, Hublin JJ. 2013. A comparison of proximal humeral cancellous bone of great apes and humans. J Hum Evol 65:29–38.
Sellers W, Pataky TC, Caravaggi P, Crompton RH. 2010. Evolutionary robotic approaches in primate gait analysis. Int J Primatol 31:321–338.
Shaw CN, Ryan TM. 2012. Does skeletal anatomy reflect adaptation to locomotor patterns? cortical and trabecular architecture in human and nonhuman anthropoids. Am J Phys Anthropol 147:187–200.
Swartz SM. 1993. The biomechanics of primate limbs. In: Gebo DL, editor. Postcranial adaptation in nonhuman primates. DeKalb: Northern Illinois University Press.
Thackeray JF, de Ruiter DJ, Berger LR, Van der Merwe NJ. 2001. Hominid fossils from Kromdraai: A revised list of specimens discovered since 1938. Ann Transvaal Mus 38:43–56.
Trussel HJ. 1979. Comment on "Picture thresholding using an iterative selection method." IEEE Trans Syst Man Cyb 9:311.
Urbanowicz M, Prejzner-Morawska A. 1972. The triceps surae in chimpanzees. Folio Morphol 31:485–493.
Vereecke EE, D'Aout K, Aerts P. 2006. The dynamics of hylobatid bipedalism: Evidence for an energy-saving mechanism? J Exp Biol 209:2829–2838.
Vereecke EE, D'Aout K, Payne R, Aerts P. 2005. Functional analysis of the foot and ankle myology of gibbons and bonobos. J Anat 206: 453–476.
White TD, Asfaw B, Beyene Y, Haile-Selassie Y, Lovejoy CO, Suwa G, WoldeGabriel G. 2009. *Ardipithecus ramidus* and the paleobiology of early hominids. Science 326:75–86.
Whitehouse WJ. 1974. The quantitative morphology of anisotropic trabecular bone. J Microscopy 101:153–168.
Wolff J. 1892. Das gesetz der transformation der knochen. Springer, Berlin: Hirchwild, Berlin; (Translated as The law of bone remodeling).
Zipfel B, DeSilva JM, Kidd RS, Carlson KJ, Churchill SE, Berger LR. 2011. The foot and ankle of *Australopithecus sediba*. Science 333:1417–1420.